

Extremely narrow peaks in predissociation of sodium dimer due to rovibronic coupling

Edvardas Narevicius,^{a)} Nimrod Moiseyev,^{b)} H. R. Sadeghpour, and Lorenz S. Cederbaum^{c)}
*Institute of Theoretical Atomic, Molecular, and Optical Physics, Harvard-Smithsonian Center
 for Astrophysics, Cambridge, Massachusetts 02138*

(Received 15 March 2004; accepted 25 May 2004)

In sodium dimer the $2^3\Pi_g$, $3^3\Pi_g$, and $4^3\Sigma_g^+$ electronic states are coupled; the coupling of the two $3^3\Pi_g$ states is due to vibrational motion while the nonadiabatic interaction between the $3^3\Sigma_g^+$ and the $3^3\Pi_g$ states—in particular, the $3^3\Pi_g$ state—is mediated by rotational interaction. The resulting vibronic problem is studied in some detail. The bound vibrational states of the $3^3\Pi_g$ and $4^3\Pi_g^+$ states lie in the dissociation continuum of the $2^3\Pi_g$ state and become resonances due to the prevailing nonadiabatic coupling. The resonances are calculated using the complex scaling method and the available *ab initio* adiabatic potential energy curves. It is demonstrated that the resonances associated with rotational nonadiabatic coupling are narrower by several orders of magnitude than those that emerge from the vibrational nonadiabatic coupling. The predissociation cross section is computed and compared with experiment. © 2004 American Institute of Physics.
 [DOI: 10.1063/1.1773171]

I. INTRODUCTION

Experimental studies of sodium dimer predissociation in the energy region between $3s+3d$ and $3s+4p$ atomic dissociation limits have been reported.^{1–3} A large number of peaks in the experimental predissociation cross section (measured as atomic fluorescence spectrum) have been associated with the resonance states of sodium dimer.

Lifetimes of the identified resonance states varied within several orders of magnitude indicating their different nature. Some of the short-lived Na_2 resonance states have been attributed to the predissociated $3^3\Pi_g$ vibrational levels by Liu *et al.*¹ The $2^3\Pi_g$ and $3^3\Pi_g$ electronic states adiabatically dissociate to the $3s+3d$ and $3s+4p$ atomic limits, respectively. These two electronic potential surfaces have avoided crossing in the region of the inner turning point, $R \sim 5$ a.u. Thus a number of bound states of $3^3\Pi_g$ interact with the continuum of the $2^3\Pi_g$ and become metastable short living resonance states.

The appearance of the long lived resonance states in the experimental cross section was explained by Li *et al.*² They suggested that the vibrational levels of $4^3\Sigma_g^+$ above the $3s+3d$ limit are predissociated by the continuum of the $2^3\Pi_g$ via the resonance states of the $3^3\Pi_g$. Fermi golden rule approximation has been used to estimate lifetimes of the resonances states.

In this article, we focus our attention on demonstrating that the complicated structure observed in photodissociation experiments on Na_2 can be explained by nonadiabatic coupling of potential energy curves (PECs). The computations are performed using the complex scaling method which pro-

vides not only the energies and widths of the resonance states, but also allows one to classify these states by inspecting the nodal structure of the computed corresponding wave functions.⁴ Specifically, we calculate the resonance energies and lifetimes as well as the predissociation cross section by taking into account both the vibronic coupling between the $2^3\Pi_g$ and $3^3\Pi_g$ and rotational-electronic coupling between $3^3\Pi_g$ and $4^3\Sigma_g^+$ states. We show here that this subset of the full interaction is sufficient to obtain both broad and narrow resonance states associated with the predissociating levels of $3^3\Pi_g$ and $4^3\Sigma_g^+$, respectively.

Our calculations are numerically exact and do not involve perturbative approximations. We obtain *all* the resonance states associated with the physical system under study by using the complex generalization of variational principle.⁵ The resonance states were later used to construct the predissociation cross section based on the formalism of non Hermitian scattering theory.⁶ Theoretical calculations involving rotational-electronic coupling between different electronic states of triatomic molecules were performed earlier by Cederbaum's group.^{7,8}

II. POTENTIAL ENERGY CURVES

We begin with the potential energy curves of the electronic states involved in predissociation. Initially, the intermediate, $v=14$, $J=14$, state is prepared by a pump laser pulse in the $b^3\Pi_u$ electronic state which dissociates to the $3s+3p$ limit as shown in Fig. 1. The minimal set of electronic states that can describe the predissociation resonances due to direct (electronic) and indirect (rotational-electronic) couplings, consists of three states $2^3\Pi_g$, $3^3\Pi_g$, and $4^3\Sigma_g^+$: The $2^3\Pi_g$ dissociates to the $3s+3d$ limit and provides the continuum states in the energy region between the $3s+3d$ and $3s+4p$ dissociation thresholds. Both the $3^3\Pi_g$ and $4^3\Sigma_g^+$ dissociate to the $3s+4p$ limit and support bound vibrational levels in the same energy range. A closer look at

^{a)}Present address: Optun Inc., 3211 Scott Blvd., Santa Clara, CA 95054.

^{b)}Permanent address: Department of Chemistry and Minerva Center of Non-linear Physics in Complex Systems, Technion—Israel Institute of Technology, Haifa 32000, Israel.

^{c)}Permanent address: Theoretische Chemie, Physikalisch-Chemisches Institut, Universität Heidelberg, D-69120 Heidelberg, Germany.

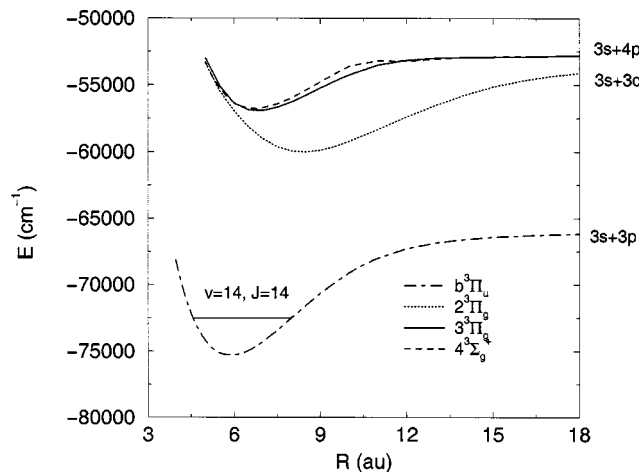


FIG. 1. Potential energy curves of electronic states involved in the predissociation experiment. The $2^3\Pi_g$ and $3^3\Pi_g$ curves dissociating to the $3s+3d$ and $3s+4p$ atomic limits are diabatic curves constructed from adiabatic *ab initio* data (Refs. 9 and 10). The energy origin is at the dissociation limit for producing two Na^+ ions.

the adiabatic $3^3\Pi_g$ and $4^3\Sigma_g^+$ PECs in the region of the inner turning point reveals that there is an avoided crossing at about $R=5.44$ a.u. The estimated closest approach adiabatic energy difference at the avoided crossing is 376 cm^{-1} (Liu *et al.*¹ used the value of 300 cm^{-1}). Assuming a slow dependence of the diabatic electronic coupling (Gaussian shape with full width at half maximum of 3 a.u. centered at $R_c=5.44$ a.u.), we performed the transformation of adiabatic potential energy curves to the diabatic PEC set. The resulting diabatic PECs for both the $2^3\Pi_g$ and $3^3\Pi_g$ states are presented in Fig. 1. In order to simplify the application of complex scaling method the *ab initio* PECs were fitted to analytic functions (we choose a sum of Morse oscillator and two Lorentzian functions).

III. PREDISSOCIATION DUE TO VIBRONIC INTERACTION OF $2^3\Pi_g$ AND $3^3\Pi_g$ STATES

First, we calculate the Na_2 predissociating resonance levels and spectrum by taking into account the vibronic coupling between the $2^3\Pi_g$ and $3^3\Pi_g$ states. The vibrational levels of the $3^3\Pi_g$ PEC, above the $3s+3d$ dissociation limit, become resonance states due to the diabatic coupling to the continuum of the $2^3\Pi_g$ PEC. The two-coupled electronic state Schrödinger equations are given by

$$\begin{pmatrix} H(2^3\Pi_g) & H_{el}(2^3\Pi_g, 3^3\Pi_g) \\ H_{el}(3^3\Pi_g, 2^3\Pi_g) & H(3^3\Pi_g) \end{pmatrix} \begin{pmatrix} \phi_{2^3\Pi_g}^E(R) \\ \phi_{3^3\Pi_g}^E(R) \end{pmatrix} = E \begin{pmatrix} \phi_{2^3\Pi_g}^E(R) \\ \phi_{3^3\Pi_g}^E(R) \end{pmatrix}, \quad (1)$$

where $H(2^3\Pi_g, 3^3\Pi_g) = T + V_{2^3\Pi_g, 3^3\Pi_g}^d + H_{rot}$ is the sum of electronic and rotational, $H_{rot} = \hbar^2 J(J+1)/(2\mu R^2)$, Hamiltonian, T is the nuclear kinetic energy operator, $V_{2^3\Pi_g, 3^3\Pi_g}^d$ are the diabatic PECs, and $H_{el}(2^3\Pi_g, 3^3\Pi_g)$ is the diabatic electronic coupling also de-

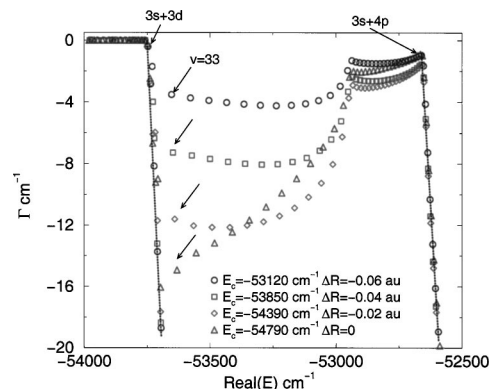


FIG. 2. The complex energy spectra of $3^3\Pi_g$ and $2^3\Pi_g$ electronically coupled states obtained by varying the avoided crossing point energy. The quantity ΔR indicates the change of the crossing point compared to the original *ab initio* data. The rotating continua are denoted by dotted lines. The resonance positions and lifetimes obtained for the $\Delta R = -0.02$ a.u. show reasonable agreement with the experimental results.

noted by $V_{el}^d(R)$. We employed the complex scaling method, $\tilde{R} = (R - R_0)\exp(i\theta) + R_0$, to obtain resonance energies and wave functions, where θ is the complex rotation parameter and $R_0 = 6.58$ a.u. is the rotation origin chosen to coincide with the minimum of the $3^3\Pi_g$ PEC. Within the complex scaling method resonance phenomena is described by the discrete part of the complex-scaled Hamiltonian spectrum. Moreover, a resonance state is associated with a single square integrable function, rather than a collection of continuum eigenstates of the conventional Hermitian Hamiltonian.⁴

Complex eigenvalues of Eq. (1) presented in Fig. 2 (see open triangles only) fall into several classes. Eigenstates that are below the $3s+3d$ dissociation limit are the bound vibrational levels of $2^3\Pi_g$ and $3^3\Pi_g$. Continua of the $2^3\Pi_g$ and $3^3\Pi_g$ are rotated into the complex energy plane by the angle 2θ around the $3s+3d$ and $3s+4p$ thresholds, respectively. Between the two dissociation limits a number of discrete θ -invariant resonance states are exposed. They are associated with the vibrational levels in the $3^3\Pi_g$ PEC and decay to the $3s+3d$ continuum. The real part of the complex eigenvalue, $E - i\Gamma/2$ gives the resonance position, while the complex part is related to the decay probability $w = \Gamma/\hbar$. Note that a series of densely spaced resonances appear close to the $3s+4p$ dissociation threshold. These resonances are located between 53 000 and 52 800 wave numbers in Fig. 2 and are due to the shape of the $3^3\Pi_g$ adiabatic potential energy curve near dissociation.

The calculated resonance width for the state, that can be associated with the $v=33$ vibrational level of $3^3\Pi_g$, is 16 cm^{-1} . Liu *et al.*¹ measured the linewidth of the same resonance state and obtained the value of 22 cm^{-1} . Based on perturbation theory, they estimated the resonance width to be 42 cm^{-1} . Although the width of the $v=33$ resonance state that has been obtained by our complex-variational calculations is in a good agreement with the experimental results, we found that the widths at higher energies ($v > 33$) deviate considerably from the experimental values (see Liu *et al.*,¹ Fig. 1). The widths of the first 12 ($33 < v < 44$) calculated

resonances decrease monotonically with energy whereas the widths of the corresponding peaks in the experimental cross section do not change appreciably. We found out that this disagreement may be corrected by tuning the energy position of the diabatic electronic potential crossing point between the two $3^3\Pi_g$ states as was first proposed by Liu *et al.*¹ Note, that the value of the crossing $R_c = 5.44$ a.u. is close to the first grid point at $R = 5$ a.u. in the *ab initio* potential energy data and hence not reliable. We tuned the energy of the crossing point by shifting the $3^3\Pi_g$ diabatic PEC with respect to the $2^3\Pi_g$ PEC in coordinate space. Complex energy spectra obtained for different values of the crossing point energy are presented in Fig. 2. The shift of the avoided crossing energy to higher values causes the calculated resonance width to decrease. This is in contradiction with earlier assumptions of Liu *et al.*¹ The decrease in the resonance width is accompanied by the qualitative change in the resonance structure behavior. For a higher (than that estimated from *ab initio* data) crossing point energy, $E_c = 54\,390$ cm⁻¹ (diamonds in Fig. 2), the width of the first ten resonance states is about constant, in agreement with the experimental results.

We have confirmed here that the resonance lifetime is sensitive to the energy at the avoided crossing, as was pointed out by Liu *et al.*,¹ and that by fitting the calculated resonance lifetimes to the peak widths in the experimental predissociation cross section, one can estimate the energy at the crossing more accurately than from the *ab initio* data. Shifting the potential energy curve is not the most accurate way to tune the avoided crossing point position. Changing the steepness of the repulsive wall at small internuclear distances is more physically sound, however because our intention here is not to find an exact agreement with experiment, we proceed with the *ab initio* PECs as calculated by Magnier *et al.*^{9,10}

Upon obtaining the resonance eigenvalues and eigenfunctions, it is straightforward to calculate the photodissociation cross section.^{11,12} The photodissociation cross section can be written as the half-collision Lippman–Schwinger equation

$$\sigma(E) = |\langle \Psi_i | 1 + GV | \Psi_f \rangle|^2, \quad (2)$$

where G is the Green operator $G = 1/(E - H)$ associated with the full Hamiltonian H ,

$$\sigma(E) = \left| \sum_k \frac{(\Psi_i | \phi_k)(\phi_k | V | \Psi_f)}{E - E_k} \right|^2, \quad (3)$$

and $(E_k$ and $|\phi_k\rangle$), respectively, are the eigenvalues and eigenvectors of the full Hamiltonian.

In the experiment, the initial state is prepared on the two triplet Π_g states by applying a laser field to the $v = 14$, $J = 14$ intermediate level of $b^3\Pi_u$,

$$\Psi_i = \begin{pmatrix} |b^3\Pi_u v=14 J=14\rangle \\ \mu_r |b^3\Pi_u v=14 J=14\rangle \end{pmatrix}. \quad (4)$$

The first and second elements of the vector stand for the portion of the wave function excited to the $3^3\Pi_g$ and $2^3\Pi_g$ electronic states, respectively, and μ_r is the ratio between the transition dipole moments (we assume coordinate independent transition dipole moment). The value of μ_r is chosen to

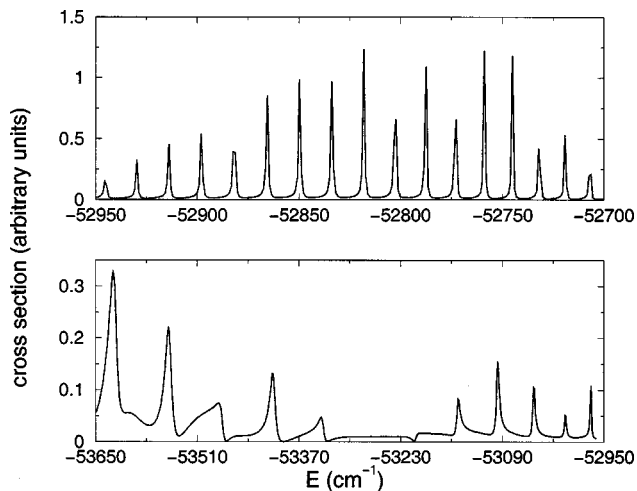


FIG. 3. Calculated predissociation cross section of $3^3\Pi_g$ levels electronically coupled to $2^3\Pi_g$ continuum.

fit the experimental absorption peaks. Since we are interested in calculating the photodetachment cross section in the energy region between the $3s+3d$ and $3s+4p$ dissociation limits, the only channel open for dissociation is the $2^3\Pi_g$ continuum. Therefore the final state vector consists of continuum wave function of $2^3\Pi_g$ only. To simplify the calculations we approximate the final vector by taking the complex scaled outgoing wave of energy $E = \hbar^2 k^2 / (2\mu)$ instead,

$$\Psi_f = \begin{pmatrix} 0 \\ \sqrt{\frac{1}{k}} e^{ik((R-R_0)\exp(i\theta)+R_0)} \end{pmatrix}. \quad (5)$$

The photodetachment cross section presented in Fig. 3, reproduces correctly the positions and the asymmetric line broadening of the peaks. The reversal of Fano's line shape asymmetry parameter q happens at the minimum of the cross section $E = -53\,300$ cm⁻¹. This line shape modulation for the molecular systems was first predicted by Cornett *et al.*¹³ Our results presented in Fig. 3 are in a good agreement with theoretical results obtained by Kimura *et al.*³ Note, however, that the calculations performed by Kimura *et al.* do not provide resonance positions and widths explicitly.

IV. PREDISSOCIATION DUE TO ROVIBRONIC INTERACTION OF $2^3\Pi_g$, $3^3\Pi_g$, AND $4^3\Sigma_g^+$ STATES

This simple model of two electronically coupled $3^3\Pi_g$ states does not account for the narrow features that appear on top of the broad ones in the experimental photodissociation cross section. One of the possible mechanisms that may lead to the presence of long-lived resonance states is the interaction of the $3^3\Pi_g$ states with the $4^3\Sigma_g^+$ state. On symmetry grounds, the coupling between the Σ and Π states cannot be the direct electrostatic coupling. Bearing in mind that the total angular momentum is large ($J = 15$), rovibronic coupling has to be considered. The total molecular Hamiltonian is given by

$$H = H_{el} + H_{vib} + H_{rot}, \quad (6)$$

where H_{el} is the electronic Hamiltonian and

$$H_{vib} + H_{rot} = -\frac{1}{2\mu} \frac{\partial^2}{\partial R^2} + \frac{1}{2\mu R^2} (\mathbf{J} - \mathbf{L} - \mathbf{S})^2, \quad (7)$$

where \mathbf{J} , \mathbf{L} , and \mathbf{S} are the total, the electronic orbital and spin angular momenta, respectively. Since the projection of the nuclear angular momentum on the molecule-fixed axis is zero ($J_z - L_z - S_z = 0$), the rotational Hamiltonian in Eq. (7) can be rewritten,

$$H_{rot} = \frac{1}{2\mu R^2} \{[(\mathbf{J}^2 - J_z^2) + (\mathbf{L}^2 - L_z^2) + (\mathbf{S}^2 - S_z^2)] + (L^+ S^- + L^- S^+) - (J^+ L^- + J^- L^+) - (J^+ S^- + J^- S^+)\}. \quad (8)$$

Represented in the electronic diabatic basis $H_{el} + H_{vib}$ leads to the vibronic Hamiltonian. It is convenient to choose a diabatic electronic-rotational basis which is suitable to represent also the rotational part of the Hamiltonian. The resulting Hamiltonian matrix operator is our rovibronic Hamiltonian. Note that four “good quantum” numbers can be assigned to the adiabatic electronic states; the electronic quantum number n (denoted by indices 2, 3, and 4 in our case): It is actually not a quantum number but an index. Λ , the projection of the electronic orbital momentum on the molecular z axis (± 1 for the ${}^3\Pi_g$ states and 0 for the ${}^3\Sigma_g^+$ state); and Σ , the projection of the electronic spin on the molecular axis (0, ± 1 in all three states). The fourth quantum number is, of course, $\Omega = \Lambda + \Sigma$, the projection of the total angular momenta J on the z axis.

The rovibronic Hamiltonian can be constructed using 15 electronic-rotational states associated with the $2\ 3\Pi_g$, $3\ 3\Pi_g$ and $4\ 3\Sigma_g^+$ symmetries. For the ${}^3\Pi_g$ states, $\Lambda = \pm 1$, $S = 1$, and $\Sigma = 1, 0, -1$. For $\Lambda = 1$, Ω can assume values 0, 1, and 2. The set of three electronic-rotational wave functions $\{\phi^{\Pi}(n, \Lambda = 1)\}$ possesses the following set of good quantum numbers:

$$\begin{aligned} \phi_0^{\Pi} &= |n, J, \Omega = 0, L, \Lambda = 1, S, \Sigma = -1\rangle, \\ \phi_1^{\Pi} &= |n, J, \Omega = 1, L, \Lambda = 1, S, \Sigma = 0\rangle, \\ \phi_2^{\Pi} &= |n, J, \Omega = 2, L, \Lambda = 1, S, \Sigma = 1\rangle. \end{aligned} \quad (9)$$

Three more electronic-rotational functions $\{\phi^{\Pi}(n, \Lambda = -1)\}$ correspond to the values of $\Lambda = -1$ and $\Omega = 0, -1, -2$. In total, there are six rotational symmetry levels associated with each ${}^3\Pi$ state $n = 2$ and $n = 3$. The total angular momentum is $J = 15$ and the electronic spin angular momentum is $S = 1$. As discussed below, we assume that L is a good quantum number where $L = 1$ for the ${}^3\Pi_g$ state and $L = 2$ for the ${}^3\Sigma_g^+$ state. For the $4\ 3\Sigma_g^+$ state, $\Lambda = 0$, $S = 1$, and $\Sigma = -1, 0, 1$. The corresponding set of three rotational-electronic wave functions, $\{\phi^{\Sigma}\}$ has the following quantum numbers:

$$\begin{aligned} \phi_{-1}^{\Sigma} &= |n, J, \Omega = -1, L, \Lambda = 0, S, \Sigma = -1\rangle, \\ \phi_0^{\Sigma} &= |n, J, \Omega = 0, L, \Lambda = 0, S, \Sigma = 0\rangle, \\ \phi_1^{\Sigma} &= |n, J, \Omega = 1, L, \Lambda = 0, S, \Sigma = 1\rangle. \end{aligned} \quad (10)$$

The total angular momentum is $J = 15$, electronic spin angular momentum is $S = 1$, and electronic orbital momentum is $L = 2$.

The matrix elements of the full Hamiltonian in Eq. (7) in the representation of 15 electronic-rotational wave functions can be easily calculated using the selection rules and the properties of raising/lowering operators [see, for instance, Lefebvre-Brion and Field for details (Ref. 14)]. We may also assume that the $(L^2 - L_z^2)$ diagonal Hamiltonian term has been already included in the calculations of the adiabatic PECs. We, however, took this term into consideration in our calculations assuming that L is a good quantum number ($L = l_1 + l_2$, where l_1 and l_2 are the electronic orbital momentum of atomic orbitals used in the construction of the asymptotic electronic wave functions). Following this assumption $L = 1$ for the $3\ 3\Pi_g$ and the $4\ 3\Sigma_g^+$ states and $L = 2$ for $2\ 3\Pi_g$ state.

It is convenient to represent the 15×15 Hamiltonian as a tri-diagonal block matrix. The block size is 3×3 and is associated with $\Sigma = -1, 0, +1$ states. Each block corresponds to one of the five available electronic-rotational wave function sets $\{\phi^{\Pi}(n = 2, \Lambda = 1)\}$, $\{\phi^{\Pi}(n = 2, \Lambda = -1)\}$, $\{\phi^{\Pi}(n = 3, \Lambda = 1)\}$, $\{\phi^{\Pi}(n = 3, \Lambda = -1)\}$, and $\{\phi^{\Sigma}(n = 4)\}$. Diagonal block associated with the ${}^3\Pi_g$ state can be represented in the basis set of Eq. (9) as

$$H(n\ 3\Pi^{\Lambda = \pm 1}) = \left(-\frac{1}{2\mu} \frac{\partial^2}{\partial R^2} + V_n^d(R) \right) \mathbf{I} + \frac{1}{2\mu R^2} \begin{pmatrix} d_0 & B_{0,1} & 0 \\ B_{1,0} & d_1 & B_{1,2} \\ 0 & B_{2,1} & d_2 \end{pmatrix}, \quad (11)$$

where \mathbf{I} is the unit matrix. Other matrix elements are given by

$$\begin{aligned} d_{\Omega} &= \langle \phi_{\Omega} | (\mathbf{J}^2 - J_z^2) + (\mathbf{L}^2 - L_z^2) + (\mathbf{S}^2 - S_z^2) | \phi_{\Omega} \rangle \\ &= [J(J+1) - \Omega^2 + L(L+1) - \Lambda^2 + S(S+1) - \Sigma^2], \\ B_{\Omega, \Omega'} &= \langle \phi_{\Omega} | J^+ S^- + J^- S^+ | \phi_{\Omega'} \rangle \\ &= [J(J+1) - \Omega'(\Omega' \pm 1)]^{1/2} [S(S+1) - \Sigma'(\Sigma' \pm 1)]^{1/2} \delta_{\Omega, \Omega' \pm 1} \delta_{\Sigma, \Sigma' \pm 1}. \end{aligned} \quad (12)$$

The values of quantum numbers used in Eq. (12) are defined within the set of rotational states as in Eq. (9). There are four diagonal 3×3 blocks that correspond to the ${}^3\Pi_g$ states $H(2\ 3\Pi, \Lambda = 1)$, $H(2\ 3\Pi, \Lambda = -1)$, $H(3\ 3\Pi, \Lambda = 1)$, and $H(3\ 3\Pi, \Lambda = -1)$. The vibrational wave functions, employed in the construction of the matrix elements, are obtained by diagonalizing the corresponding molecular Hamiltonian $T + V_n^d(R) + \hbar^2 J(J+1)/(2\mu R^2)$ with $J = 15$. We used the Colbert-Miller discrete-variable-representation approach¹⁵ with 5000 grid points and a box size of 20 a.u. A cutoff in energy of -0.2 a.u. was chosen to reduce the size of the Hamiltonian matrix without compromising the numerical accuracy. As a result, the vibrational basis set size for the $2\ 3\Pi_g$ and $3\ 3\Pi_g$ states was 313 and 285 functions, respectively (instead of 5000).

The fifth diagonal block of the full Hamiltonian matrix corresponds to the $4^3\Sigma_g^+$ state and is given by

$$H(n^3\Sigma) = \left(-\frac{1}{2\mu} \frac{\partial^2}{\partial R^2} + V_n^d(R) \right) \mathbf{I} + \frac{1}{2\mu R^2} \begin{pmatrix} d_{-1} & B_{-1,0} & 0 \\ B_{0,-1} & d_0 & B_{0,1} \\ 0 & B_{1,0} & d_1 \end{pmatrix}, \quad (13)$$

where matrix elements d_Ω and $B_{\Omega,\Omega'}$ are calculated by substituting the quantum numbers given in Eq. (10) into Eq. (12). The vibrational basis set size used for the $4^3\Sigma_g^+$ state was 283.

We have assumed earlier that the electronic configuration of the $2^3\Pi_g$ state involves 3s and 3d atomic orbitals. This is rigorously correct only in the asymptotic limit. Similarly the electronic configurations of the $3^3\Pi_g$ and the $4^3\Sigma_g^+$ states include 3s and 4p orbitals. This implies that in our scheme there is no electronic-rotational coupling between the $2^3\Pi_g$ state and the $3^3\Pi_g$ or $4^3\Sigma_g^+$ states, since there is no operator in the rotational Hamiltonian equation (7), that changes the principal quantum number. However there is an electrostatic (radial) coupling between the $2^3\Pi_g$ and $3^3\Pi_g$ PECs and it is nonvanishing only between electronic-rotational states having the same set of rotational good quantum numbers. The off-diagonal 3×3 block of the full Hamilton matrix [see Eq. (17) below] that represents the electrostatic coupling can be expressed using the set of $^3\Pi$ electronic-rotational wave functions given in Eq. (9) as

$$H_{el}(n^3\Pi^\Lambda, n^3\Pi^\Lambda) = \begin{pmatrix} V_{el}^d(R) & 0 & 0 \\ 0 & V_{el}^d(R) & 0 \\ 0 & 0 & V_{el}^d(R) \end{pmatrix}, \quad (14)$$

$$\begin{pmatrix} H(2^3\Pi_g^1) & H_{el}(2^3\Pi_g^1, 3^3\Pi_g^1) & 0 & 0 & 0 \\ H_{el}(3^3\Pi_g^1, 2^3\Pi_g^1) & H(3^3\Pi_g^1) & H_{rot}(3^3\Pi_g^1, 4^3\Sigma_g^+) & 0 & 0 \\ 0 & H_{rot}(4^3\Sigma_g^+, 3^3\Pi_g^1) & H(4^3\Sigma_g^+) & H_{rot}(4^3\Sigma_g^+, 3^3\Pi_g^{-1}) & 0 \\ 0 & 0 & H_{rot}(3^3\Pi_g^{-1}, 4^3\Sigma_g^+) & H(3^3\Pi_g^{-1}) & H_{el}(3^3\Pi_g^{-1}, 2^3\Pi_g^{-1}) \\ 0 & 0 & 0 & H_{el}(2^3\Pi_g^{-1}, 3^3\Pi_g^{-1}) & H(2^3\Pi_g^{-1}) \end{pmatrix}. \quad (17)$$

The resulting 15×15 Hamiltonian governs the motion in the manifold of the coupled electronic and rotational states. Note that in the absence of rotational-electronic coupling the full rovibronic problem presented in Eq. (17) reduces to the 2×2 problem [Eq. (1)]. As one can see there is no direct coupling between the $4^3\Sigma_g^+$ and $2^3\Pi_g$ states, which means that the predissociation of the $4^3\Sigma_g^+$ levels is treated as a second order process in our coupling scheme. It takes place through the electronic-rotational coupling to the $3^3\Pi_g$ vibrational levels. The effect of the indirect coupling is clearly seen in the complex spectrum of the full Hamiltonian pre-

where the matrix element $V_{el}^d(R)$ is the diabatic electronic coupling.

In our approximation, both the $4^3\Sigma_g^+$ and $3^3\Pi_g$ states electronic configurations include the 3s and 4p atomic orbitals only and it is easy to calculate the electronic-rotational coupling matrix elements in the basis sets defined by Eqs. (9) and (10)

$$H_{rot}(4^3\Sigma, n^3\Pi^\Lambda) = \frac{1}{2\mu R^2} \begin{pmatrix} 0 & D_{-1,1} & C_{-1,2} \\ D_{0,0} & C_{0,1} & 0 \\ C_{1,0} & 0 & 0 \end{pmatrix}, \quad (15)$$

where the matrix elements C and D are calculated at $R = \infty$. Within the framework of the asymptotic approximation, they are given as,

$$C_{\Omega,\Omega'} = \langle \phi_\Omega^\Sigma | (J^+ L^- + J^- L^+) | \phi_{\Omega'}^\Pi \rangle = [J(J+1) - \Omega'(\Omega' \pm 1)]^{1/2} [L(L+1) - \Lambda'(\Lambda' \pm 1)]^{1/2} \delta_{\Omega,\Omega' \pm 1} \delta_{\Lambda,\Lambda' \pm 1}, \quad (16)$$

$$D_{\Omega,\Omega'} = \langle \phi_\Omega^\Sigma | (L^+ S^- + L^- S^+) | \phi_{\Omega'}^\Pi \rangle = [L(L+1) - \Lambda'(\Lambda' \pm 1)]^{1/2} [S(S+1) - \Sigma'(\Sigma' \mp 1)]^{1/2} \delta_{\Lambda,\Lambda' \pm 1} \delta_{\Sigma,\Sigma' \mp 1}.$$

The matrix elements are calculated using the quantum numbers defined in Eqs. (9) and (10). As mentioned above, we took into account the electrostatic coupling between the $2^3\Pi_g$ and $3^3\Pi_g$ states and the rotational-electronic coupling between the $3^3\Pi_g$ and $4^3\Sigma_g^+$ states. As a result the full Hamiltonian matrix is block tridiagonal. It can be schematically shown using the 3×3 blocks defined above,

sented in Fig. 4. Predissociating resonances of the $4^3\Sigma_g^+$ state have much longer lifetime as compared to the $3^3\Pi_g$ predissociation.

The energies and widths of the resonance states were obtained by diagonalizing the total 4473×4473 complex symmetric Hamiltonian matrix. Since the complex scaling method is employed again, the resonances fall into discrete part of the spectrum and are described by square integrable localized wave functions. The nodes of the resonance wave functions can be counted facilitating the classification of resonance states.

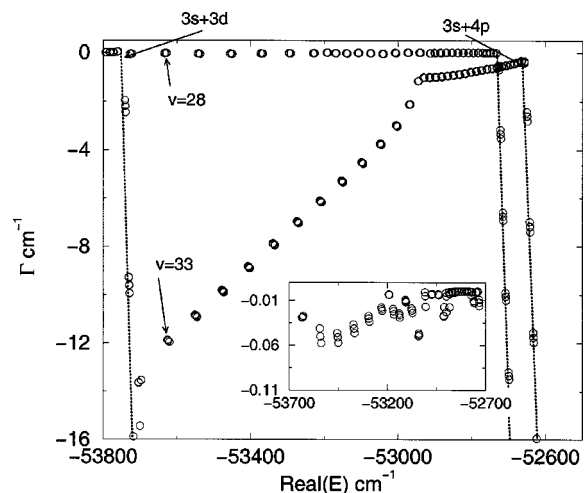


FIG. 4. The complex energy spectrum of vibrationally coupled $3^3\Pi_g$, $2^3\Pi_g$ and $4^3\Sigma_g^+$ states. The rotating continua are denoted by dotted lines. The bound states were obtained below the first $3s+3d$ threshold. The inset shows energy region with extremely narrow resonances resulting from the nonadiabatic couplings mediated by rotations.

Two groups of resonances appear in the complex energy spectrum shown in Fig. 4: (i) $3^3\Pi_g$ predissociation states similar to vibrationally unperturbed levels presented in Fig. 2 and (ii) $4^3\Sigma_g^+$ predissociation levels that have width of about 0.04 cm^{-1} (see inset in Fig. 4). The calculated width of the resonance state associated with the $v=28$ vibrational level of the $4^3\Sigma_g^+$ state is 0.06 cm^{-1} . The experimental line width² is about 0.5 cm^{-1} . A possible explanation might be that in the experiment the three rotational states of $v=28$ vibrational level of the $4^3\Sigma_g^+$ are not resolved.

The predissociation cross section was calculated within the non Hermitian scattering theory using the expression of Eq. (2). The initial state was obtained by solving the Schrödinger equation for the $v=14$, $J=14$ level of the $b^3\Pi_u$ [Eq. (11)], where $V_b'(R)$ is PEC of $b^3\Pi_u$ state. Six states with different rotational symmetry properties were found. Three states associated with $\Lambda=1$ and another three with $\Lambda=-1$. That is there are six different possibilities for the construction of the initial state. Similarly, the final state was chosen to be the continuum level of the $2^3\Pi_g$ PEC at a given energy. In order to simplify the calculations, we have approximated the final vector by the complex scaled outgoing wave at energy $E=\hbar^2k^2/(2\mu)$ corresponding to one of the six rotational states, as described in Eq. (9). Therefore, there are 36 different possible transitions from the initial to the final states. The total predissociation cross section presented in Fig. 5 is the sum of all the possible combinations of dipole excitations from the initial to the final states. As one observes, the predissociation resonances of the $4^3\Sigma_g^+$ state give rise to numerous narrow peaks in the cross section. Their classification can be easily done based on the full Hamiltonian spectrum calculations and corresponding complex scaled resonance wave functions.

V. CONCLUSION

We have shown here that the experimental predissociation cross section of sodium dimer in the energy region be-

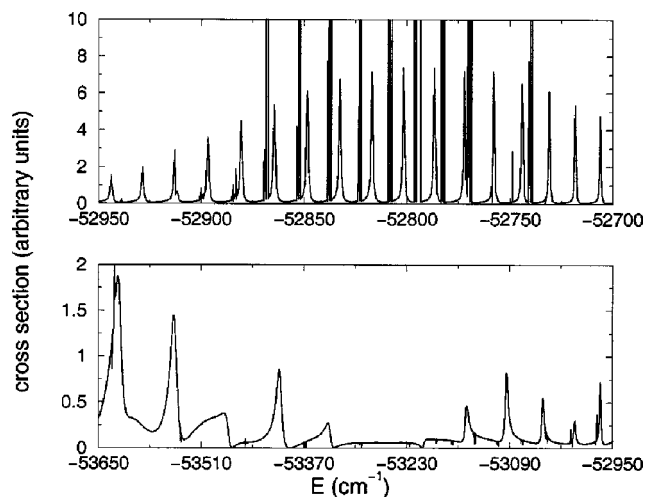


FIG. 5. Calculated predissociation cross section of $3^3\Pi_g$ and $4^3\Sigma_g^+$ levels directly and indirectly coupled to the continuum of $2^3\Pi_g$, showing the extremely narrow peaks which are associated with the resonances shown in the inset Fig. 4.

tween $3s+3d$ and $3s+4p$ atomic dissociation limits can be quite accurately reproduced by taking into account the rovibronic coupling between three potential energy curves; the $2^3\Pi_g$, $3^3\Pi_g$, and $4^3\Sigma_g^+$. Vibronic coupling between $2^3\Pi_g$ and $3^3\Pi_g$ states gives rise to short-lived predissociation resonances seen as broad peaks in the experimental cross section. Rovibronic coupling between the $4^3\Sigma_g^+$ levels and $3^3\Pi_g$ states leads to the formation of long-lived predissociating resonances. Although our coupling scheme is somewhat simplified—we do not have *ab initio* electronic wave functions to estimate the exact coupling—it is sufficiently physical to qualitatively reproduce the experiment.

ACKNOWLEDGMENTS

This work is supported by NSF through a grant for the Institute of Theoretical Atomic, Molecular, and Optical Physics at Harvard University and Smithsonian Astrophysical Observatory. The authors acknowledge Hélène Lefebvre-Brion and Robert W. Field for most helpful discussions and comments.

¹Y. Liu, J. Li, H. Gao, Li Li, R. W. Field, and A. M. Lyyra, J. Chem. Phys. **108**, 2269 (1998).

²J. Li, Y. Liu, and H. Chen, J. Chem. Phys. **108**, 7707 (1998).

³Y. Kimura, H. Kato, P. Yi, M. Song, Y. Liu, and Li Li, Phys. Rev. A **67**, 062701 (2003).

⁴N. Moiseyev, Phys. Rep. **302**, 211 (1998).

⁵N. Moiseyev, P. R. Certain, and F. Weinhold, Mol. Phys. **36**, 1613 (1978).

⁶U. Peskin and N. Moiseyev, J. Chem. Phys. **97**, 6443 (1992).

⁷M. Mayer and L. S. Cederbaum, J. Chem. Phys. **105**, 4938 (1996).

⁸M. Mayer, L. S. Cederbaum, and H. Köppel, J. Chem. Phys. **104**, 8932 (1996).

⁹S. Magnier, Ph.D. thesis, Université de Paris-Sud, Centre d'Orsay, 1993.

¹⁰S. Magnier, Ph. Millié, O. Dulieu, and F. Masnou-Seeuws, J. Chem. Phys. **98**, 7113 (1993).

¹¹E. Narevicius and N. Moiseyev, J. Chem. Phys. **113**, 6088–6095 (2000).

¹²E. Engdahl, T. Maniv, and N. Moiseyev, J. Chem. Phys. **88**, 5864 (1988).

¹³S. T. Cornett, H. R. Sadeghpour, and M. J. Cavagnero, Phys. Rev. Lett. **82**, 2488 (1999).

¹⁴H. Lefebvre-Brion and R. W. Field, *Perturbations in the Spectra of Diatomic Molecules* (Academic, New York, 1986).

¹⁵D. T. Colbert and W. H. Miller, J. Chem. Phys. **96**, 1982 (1992).